

bradscholars

Active distribution networks planning with high penetration of wind power

Item Type	Article
Authors	Mokryani, Geev;Hu, Yim Fun;Pillai, Prashant;Rajamani, Haile S.
Citation	Mokryani G, Hu YF, Pillai P et al (2017) Active distribution networks planning with high penetration of wind power. Renewable Energy. 104: 40-49.
DOI	https://doi.org/10.1016/j.renene.2016.12.007
Rights	© 2017 Elsevier. Reproduced in accordance with the publisher's self-archiving policy. This manuscript version is made available under the CC-BY-NC-ND 4.0 license (http://creativecommons.org/licenses/by-nc-nd/4.0/)
Download date	2026-05-14 03:41:33
Link to Item	http://hdl.handle.net/10454/10976

The University of Bradford Institutional Repository

<http://bradscholars.brad.ac.uk>

This work is made available online in accordance with publisher policies. Please refer to the repository record for this item and our Policy Document available from the repository home page for further information.

To see the final version of this work please visit the publisher's website. Access to the published online version may require a subscription.

Link to publisher version: <http://dx.doi.org/10.1016/j.renene.2016.12.007>

Citation: Mokryani G, Hu YF, Pillai P et al (2017) Active distribution networks planning with high penetration of wind power. *Renewable Energy*. 104: 40-49.

Copyright statement: © 2017 Elsevier. Reproduced in accordance with the publisher's self-archiving policy. This manuscript version is made available under the [CC-BY-NC-ND 4.0 license](https://creativecommons.org/licenses/by-nc-nd/4.0/).



Active Distribution Networks Planning with High Penetration of Wind Power

Geev Mokryani, Yim Fun Hu, Prashant Pillai and Haile-Selassie Rajamani

School of Electrical Engineering and Computer Science, University of Bradford, Bradford BD7 1 DP, UK

Email: g.mokryani@bradford.ac.uk, y.f.hu@bradford.ac.uk, p.pillai@bradford.ac.uk, h.s.rajamani@bradford.ac.uk

Abstract –In this paper, a stochastic method for active distribution networks planning within a distribution market environment considering multi-configuration of wind turbines is proposed. Multi-configuration multi-scenario market-based optimal power flow is used to maximize the social welfare considering uncertainties related to wind speed and load demand and different operational status of wind turbines (multiple-wind turbine configurations). Scenario-based approach is used to model the abovementioned uncertainties. The method evaluates the impact of multiple-wind turbine configurations and active network management schemes on the amount of wind power that can be injected into the grid, the distribution locational marginal prices throughout the network and on the social welfare. The effectiveness of the proposed method is demonstrated with 16-bus UK generic distribution system. It was shown that multi-wind turbine configurations under active network management schemes, including coordinated voltage control and adaptive power factor control, can increase the amount of wind power that can be injected into the grid; therefore, the distribution locational marginal prices reduce throughout the network significantly.

Index Terms — Wind power, active network management, social welfare, market-based optimal power flow, distribution network operators, distribution locational marginal prices.

Nomenclature

A. Sets and Indices

i, j	Index of system buses running from 1 to NB
w	Index of wind turbine
G	Index of substation

D	Index of loads
t	Index of energy block offered by wind turbines running from 1 to NT
q	Index of energy bids submitted by loads running from 1 to NQ
s	Index of scenarios running from 1 to NS
c	Index of configurations running from 1 to NC
y	Index of years running from 1 to NY

B. Variables

$(P/Q)_{i,t,s,c,y}^w$	Active/reactive power generated by wind turbines at bus i , block t , scenario s , configuration c and year y in MW/MVAr
$(P/Q)_{i,t,c,y}^G$	Active/reactive power at substation, block t , configuration c and year y in MW/MVAr
$V_{i,s,c,y} / \delta_{i,s,c,y}$	Voltage/voltage angle at bus i , scenario s , configuration c and year y in Volt/Radian
$\phi_{i,s,c,y}^w$	Power factor angle of WTs at bus i , scenario s , configuration c and year y in radian
T_{ij}	Tap magnitude of OLTC

C. Parameters

α	Load growth rate
β	Operational status of each WT

$\beta_{i,c}$	Operational status of WTs at bus i and configuration c
c	Scale coefficient
v	Wind speed in m/s
v_m	Mean value of wind speed in m/s
v_{ci}/v_{co}	Cut-in/cut-off wind speed in m/s
v_r	Rated wind speed in m/s
π_s	Probability of state s
$(P/Q)_{i,q,s,y}^D$	Active/reactive consumption of loads at bus i , block q , scenario s , configuration c and year y in MW/MVAr
V_i^{\min} / V_i^{\max}	Min/max voltage at each bus in Volt
$\delta_i^{\min} / \delta_i^{\max}$	Min/max voltage angle at each bus
$Q_i^{w,\min} / Q_i^{w,\max}$	Min/max reactive of WTs at bus in MVAr
$P_{i,rated}^w$	WTs rated active power in MW
$\gamma_{i,s,c}^w$	Percentage of active power generated by WTs at scenario s and configuration c
$P_i^{G,\min} / P_i^{G,\max}$	Min/max active power at substation in MW
$Q_i^{G,\min} / Q_i^{G,\max}$	Min/max reactive power at substation in MVAr
$C_{i,q}^D$	Price for the energy bid q at bus i submitted by load D in £/MWh
$C_{i,t}^w$	Price for the energy selling t at bus i by WT w

	in £/MWh
$C_{i,t}^G$	Price for the energy selling t at substation in £/MWh
G_{ij} / B_{ij}	Real/imaginary part of the element in the admittance matrix corresponding to the i^{th} row and j^{th} column in mho
I_{ij}^{\max}	Maximum current flow of wires in A

I. Introduction

A. Motivation and Approach

The connection of large amounts of renewable energy sources (RES) to distribution networks introduces many technical and economic challenges to distribution network operators (DNOs). Therefore, DNOs have to develop a rational operating strategy taking into account dispatching distributed generators (DGs), interrupting loads, and purchasing power from the wholesale market while keeping the system security. DNOs, in some cases, play the retailers role which buy power on the wholesale market at volatile prices and sell it again at fixed tariffs to small consumers. DNOs and retailers are separate market entities with different purposes, networks, and sizes [1]. However, assuming that the objective of DNOs is to maximize their benefits, two different regulatory cases can be taken into account: 1) DG-owning DNO – allowed to own DG and can exploit the financial benefits brought by considering new generation as an option for the investment in distribution network, 2) Unbundled DNO – forbidden from DG ownership but can maximize benefits based on a number of incentives. European Directive 2003/54/EC defines the technical and legal existing restrictions among different market actors of European electricity markets. In particular, it forms the unbundling regulations that DNOs have to be unbundled from generation interests, thus, forbidding DNOs from DG ownership. It splits the electricity distribution from retail supply where distribution utilities are not responsible to sell power to customers [2-3]. By introducing DGs in distribution systems, the planning for investment in distribution networks to meet the future load growth and its related infrastructures can be deferred [4]. On the other hand, emerging active network management (ANM) schemes have proved to be advantageous for DNOs, compared to passive network management [5]. ANM schemes can increase the operation

of the assets of network that allow the distribution networks to accommodate more DGs within the existing infrastructure and therefore, defer or avoid expensive network upgrades. The main ANM schemes include coordinated voltage control (CVC) of on load tap changers (OLTCs) and voltage regulators, adaptive power factor control (PFC) of DGs and energy curtailment [5-7].

This paper provides a novel approach for DNOs to evaluate the amount of wind power that can be injected into the distribution network over the planning horizon considering: 1) capability curve of doubly fed induction generator (DFIG)-based wind turbines (WTs), 2) uncertainties related to the stochastic variations of wind power generation and load demand, 3) multiple-WT configurations and 4) ANM schemes including CVC and PFC. The method also characterizes the impact of the abovementioned factors on the distribution-locational marginal prices (D-LMPs). Multi-configuration multi-scenario market-based optimal power flow (MMMOPF) is utilized to maximize the social welfare (SW) considering abovementioned uncertainties. A distribution market model, called the DNO acquisition market, is presented here under a distribution market structure based on pool and bilateral contracts within DNO's control area. It is assumed that WTs and loads are owned or managed by the DG-owning DNO [8]. Here, the DNO is defined as the market operator of the DNO acquisition market, which determines the price estimation and the optimization process for the hourly acquisition of active power [9].

B. Literature Review

Lots of studies have been reported on the benefits of ANM and its applications. Some of them revealed implementations, and experiences of ANM [10-11], online ANM application [12-13], and ANM challenges for network operators [14]. The cost-benefit analysis of investments and operation costs for various combinations of ANM schemes and techno-economic evaluation are studied in [15-17] and compared with passive network management scheme. Generally, it is found that as the DG penetration increases, the investment costs of ANM schemes become more viable and justifiable. Also, several works have been carried out about the planning and operation of distribution networks with integration of DGs [18-19]. In [18], the authors proposed a cost based model to allocate DGs in distribution networks to minimize DG investment and total operation costs. In [19], a method for optimal placement of WTs in distribution networks to minimize annual energy losses has been proposed. However, these studies also did not consider the distribution market environment as well as the effect of multi DG-configurations which considerably impact the allocations and amount of connected DG capacity.

C. Contributions

The gap that this paper tries to fill is how the combination of multi-WT configurations and ANM schemes can impact on the total dispatched energy of WTs and D-LMPs within a distribution market environment. To the best of the authors' knowledge, no stochastic method for the planning of active distribution networks within a distribution market environment considering multiple-WT configurations and capability curve of DFIG-based WTs and ANM schemes has been reported in the literature. The dynamic nature of the power system operation has not been taken into account in the conventional planning studies with integration of DGs. For example, in [5-7] and [20-22], the authors have not addressed the impact on the overall DG penetration level when one or more existing DGs are absent. Moreover, the presence of a distribution market environment has not been addressed in the abovementioned studies. One of the innovative contributions of this paper is proposing a novel MMMOPF-based planning approach which considers the operational status of WTs at the planning stage, and assesses the dispatched energy of WTs considering various multi-configurations within the DNO market environment which has not been addressed so far. It also provides detailed analysis and results on how multiple-WT configurations and ANM schemes could impact the amount of wind power that can be injected into the grid as well as the D-LMPs throughout the network. Another novel contribution of the proposed method is that it can be used as a tool for DG-owning DNOs to better allocate WTs in terms of consumers' benefits and cost reduction and network constraints. It also can evaluate the contribution of DG-owning DNOs in a distribution market, including both a day-ahead and a real-time intraday schedule of WTs and load demand according to the market price.

D. Paper Organization

The rest of the paper is organized as follows. Section II explains the structure of the proposed method. Multi-WT configurations and uncertainty modeling are discussed in Sections III and IV, respectively. Problem formulation is described in Section V. Section VI presents the 16-bus UK generic distribution system (UKGDS) and simulation results. Conclusions are presented in Section VII.

II. The Structure of the Proposed Method

The stochastic variations of wind speed and load demand are modelled by Weibull and Normal probability density functions (PDFs), respectively. Then, each obtained PDF, is divided into several intervals and the probability of

falling into each interval is calculated. It is assumed that the wind speed and load demand scenarios are independent, so the scenarios are combined by multiplication of the probability of load and wind scenarios to construct the whole set of scenarios. For each combination of wind speed and load demand, different MMMOPFs are carried out to maximize the SW considering multiple-configuration of WTs and their capability curve and ANM schemes. The products of the proposed method are: the injected wind power into the network, the SW, and the D-LMPs. The following steps are carried out by the proposed method as shown in Fig.1:

- 1) Set the candidate buses according to wind speed historical data.
- 2) Define the size and speed-power curve of WTs.
- 3) Model wind speed by using Weibull PDF [23]. Divide the PDF into several intervals and calculate the probability of falling into each interval.
- 4) Model load demand by using Gaussian PDF [24] and divide the obtained PDF into different intervals then calculate the probability of each interval. The probability of the scenarios is multiplied by the bid quantities which are considered as bid quantity in the DNO acquisition market.
- 5) Calculate the probability of each scenario from the PDF of wind speed as described above then derive the PDF of WTs active power output based on Weibull PDF of wind speed and power curves of WTs. The multiplication of active power generated by WTs and the probability of the wind scenarios is considered as the offer quantity in the DNO acquisition market.
- 6) Calculate the combined generation-load scenarios as explained in Section IV.
- 7) Calculate the WTs' offer price as explained in Section VI.
- 8) For each scenario and configuration, maximize the SW by using MMMOPF over the planning horizon subject to network constraints. The DNO acquisition market formulation and the optimization problem are described in Section V.
- 9) The products of the proposed method provide injected wind power, the SW, and the D-LMPs.

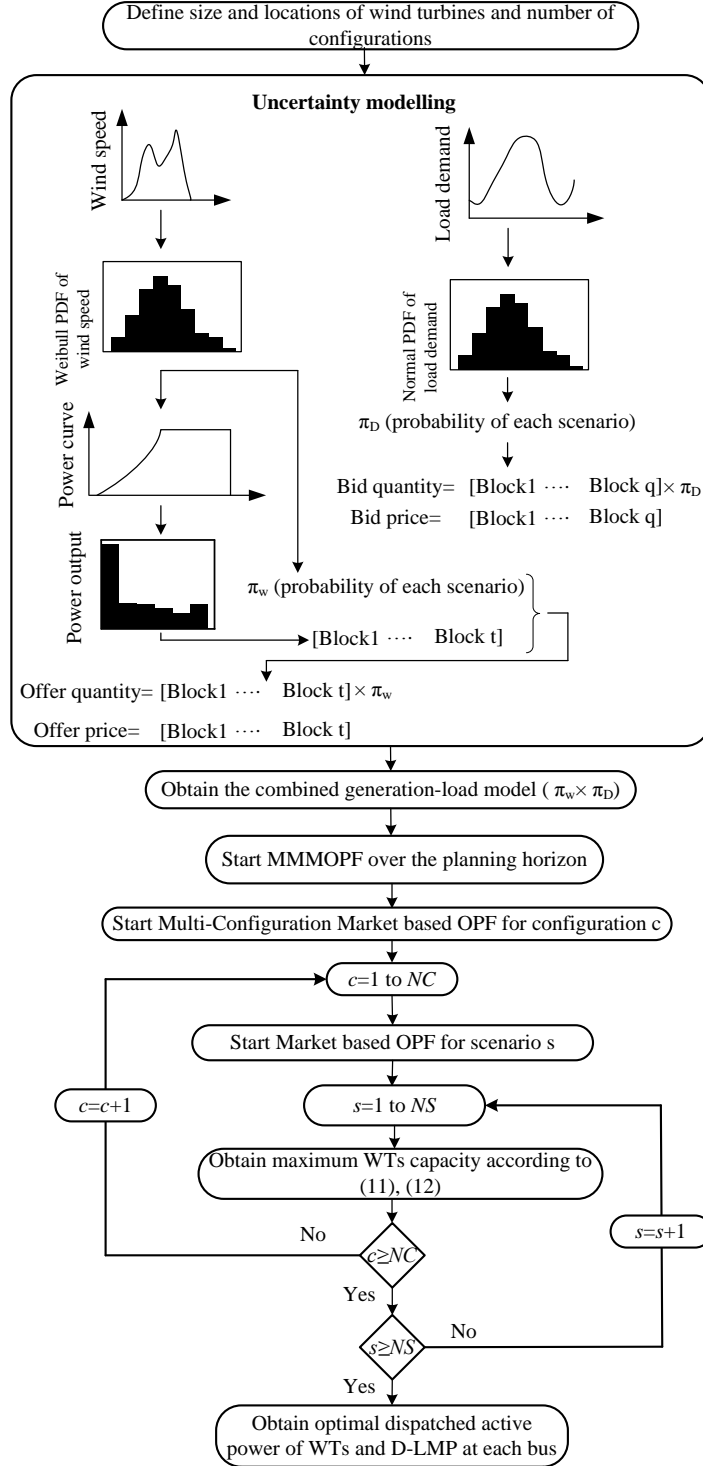


Fig.1. The structure of the proposed method

III. Multi-WT Configurations

In this paper, the MMMOPF method aims to incorporate multi-WT configurations which are defined as the operational status of WTs, and are chosen based on the DNO's decisions. The total number of all possible multi-configurations for any number of WTs can be expressed as follows:

$$1 \leq NC \leq (2^{NW} - 1) \quad (1)$$

The total configurations are referred as the number of multi-WT configurations. For example, if a system has five WTs, there will be up to 31 possible multi-WT configurations for the DNOs to choose. A binary parameter is defined to represent the operational status of WTs at i^{th} bus for configuration c . The operational status of each WT and all WTs are described in (2) and (3), respectively.

$$\beta_{i,c} = \begin{cases} 1, & \text{if a wind turbine at } i^{\text{th}} \text{ bus is operating} \\ 0, & \text{otherwise} \end{cases} \quad (2)$$

$$\beta = \begin{bmatrix} \beta_{1,w_1} & \beta_{1,w_2} & \cdots & \beta_{1,w_N} \\ \beta_{2,w_1} & \beta_{2,w_2} & \cdots & \beta_{2,w_N} \\ \vdots & \vdots & \ddots & \vdots \\ \beta_{c,w_1} & \beta_{c,w_2} & \cdots & \beta_{c,w_N} \end{bmatrix}_{(NC \times NW)} \quad (3)$$

In the proposed method, there is capacity constraint for WTs according to its operational status for each configuration which is described as follows:

$$P_{i,c}^w = \begin{cases} 0 \leq P_{i,c}^w \leq P_{i,c}^{w,\max}, & \forall \beta_{i,c} = 1 \\ 0, & \forall \beta_{i,c} = 0 \end{cases} \quad (4)$$

IV. Uncertainty Modelling

A. Wind Speed Modelling

A good expression often used to model the wind speed behavior is the Rayleigh PDF. It is a special case of Weibull PDF where the shape index is equal to 2. The Weibull PDF equation is as follows:

$$f(v) = \left(\frac{2v}{c^2}\right) \exp\left[-\left(\frac{v}{c}\right)^2\right] \quad (5)$$

where v and c are respectively the wind speed and the scale coefficient. If the mean value of the wind speed for a site is known, then the scaling index c is calculated as follows in (6) and (7).

$$v_m = \int_0^{\infty} v f(v) dv = \int_0^{\infty} \left(\frac{2v^2}{c^2}\right) \exp\left[-\left(\frac{v}{c}\right)^2\right] dv = \frac{\sqrt{\pi}}{2} c \quad (6)$$

$$c \cong 1.128 v_m \quad (7)$$

In order to incorporate the output power of WTs as a multi-state variable, the continuous PDF has been divided into states, in each state the wind speed is within specific limits. The probability of each state is calculated as follows:

$$\pi_s = \int_{v_{1,s}}^{v_{2,s}} f(v) dv \quad (8)$$

$$v_s = \frac{v_{1,s} + v_{2,s}}{2} \quad (9)$$

where $v_{1,s}$ and $v_{2,s}$ are the starting and ending points of the interval of wind speed defined in scenario s , respectively.

A typical WT output power versus rotor angular speed is shown in Fig. 2 [25]. The WT's operating strategy is to match the rotor speed to generate power continuously close to the P_{\max} points. This can be carried out with the design and operation of a variable-speed system that is utilized in the DFIG-based WFs. In order to extract the maximum possible power, the WT must operate at the peak power point for all wind speeds. This occurs at points $P_{\max,1}$, $P_{\max,2}$, $P_{\max,3}$ in wind speeds $V_{W,1}$, $V_{W,2}$, $V_{W,3}$, respectively as shown in Fig.2. The common factor among the peak power production points $P_{\max,1}$, $P_{\max,2}$, $P_{\max,3}$ is the constant high value of tip speed ratio. Therefore, the control of speed and power in wind power systems have three different regions as shown in Fig. 3, where the solid curve is the power and the dotted curves, and the rotor power coefficient (C_p) [26].

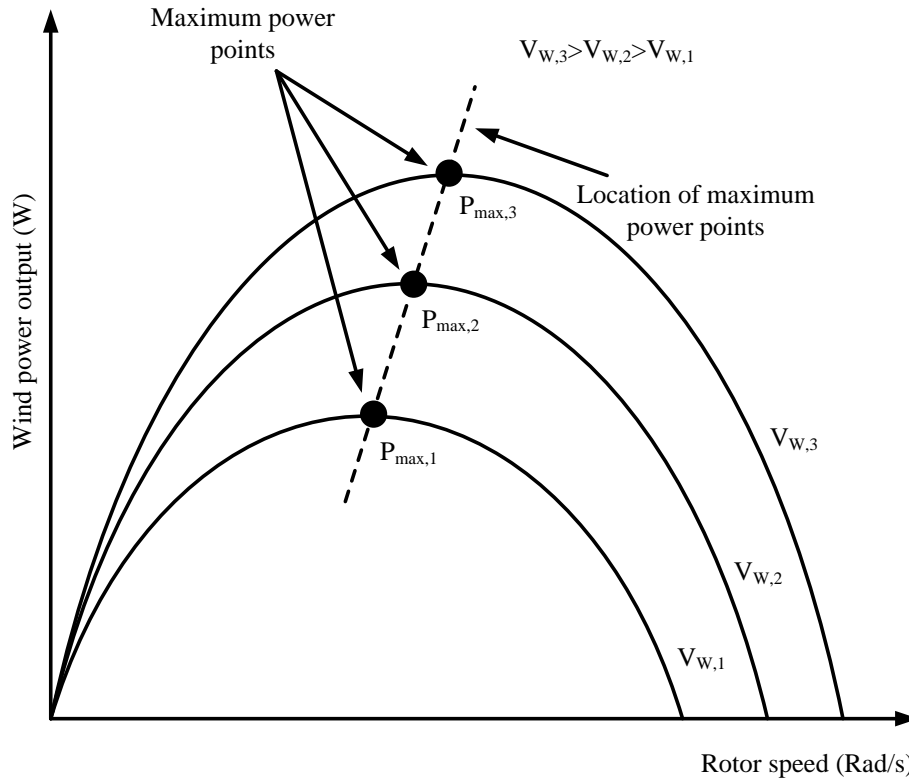


Fig.2. WT power versus rotor angular speed characteristics at different wind speeds [26]

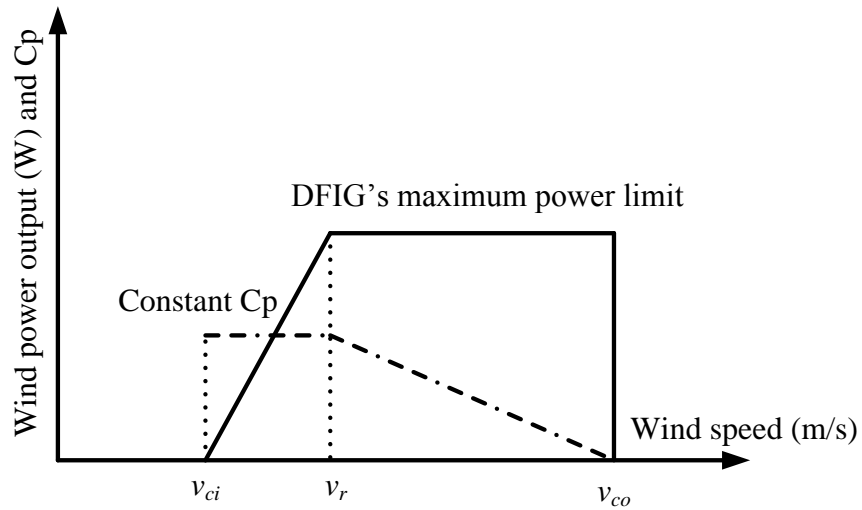


Fig.3. Three different rotor speed control regions of the system [26]

Hence, the generated power of WTs is determined using its power curve as follows:

$$P^w(v_s) = \begin{cases} 0, & 0 \leq v_s \leq v_{ci} \\ P_{rated} \times \frac{v_s - v_{ci}}{v_r - v_{ci}}, & v_{ci} \leq v_s \leq v_r \\ P_{rated}, & v_r \leq v_s \leq v_{co} \\ 0, & v_{co} \leq v_s \end{cases} \quad (10)$$

where v_{ci} , v_r and v_{co} are the cut-in speed, rated speed and cut-off speed of the wind turbine, respectively. Therefore, the wind power at bus i , scenario s and configuration c is calculated as follows:

$$0 \leq P_{i,s,c}^w \leq \gamma_{i,s,c}^w \times P_{i,rated}^w \quad (11)$$

where $\gamma_{i,s,c}^w$ is the percentage of active power generated by WTs at scenario s and configuration c . Therefore, the maximum WTs' output power is limited by the multiplication of percentage of active power generated by WTs and WTs rated power.

B. Load Modelling

Load demands are also modelled using a Normal PDF. The load demand will be divided into 6 states using the technique developed in [19], which verifies that choosing six states with different probabilities provides a reasonable trade-off between accuracy and fast numerical evaluation. Assuming peak load of $P_{i,s}^D$ in each state and load growth rate of α , the load demand $P_{i,s,y}^D$ at bus i , state s and year y , is calculated as:

$$P_{i,s,y}^D = P_{i,s}^D (1 + \alpha)^y \quad (12)$$

C. Combined Generation-Load Model

In this paper, the wind speed and the load states are assumed to be independent. So the scenarios are combined to construct the whole set of scenarios as follows:

$$\pi_s = \pi_D \times \pi_w \quad (13)$$

where π_D and π_w are the probabilities of D^{th} load and w^{th} wind states, respectively. Hence, total numbers of states are $n_D \times n_w$, where n_D and n_w are the number of individual load and wind states.

V. Problem Formulation

A. DNO Acquisition Market Formulation

Usually, electrical energy is purchased from the wholesale market and delivered to final customers by DNO. Nonetheless, due to the power system reconstructing and emerging DGs such as WTs, the business of traditional DNO is unbundled into technical and economic tasks. A DNO energy acquisition market model, called the DNO acquisition market is presented here under a distribution market structure based on pool and bilateral contracts. The DNO is defined as the market operator of the acquisition market, which determines the price estimation and the optimization process for the acquisition of active power. Loads and WTs send active power offers and bids to the DNO acquisition market in form of blocks for each hour [9, 27].

The DNO's aim is the maximization of the SW, (i.e. the maximization of the consumers' benefit function and the minimization of the costs of energy). The MMMOPF is formulated as follows:

$$\text{Maximize SW} = \sum_{s=1}^{NS} \pi_s \left\{ \sum_{q=1}^{NQ} \sum_{i=1}^{NB} \sum_{y=1}^{NY} C_{i,q}^D P_{i,q,s,y}^D - \sum_{t=1}^{NT} \sum_{i=1}^{NB} \sum_{c=1}^{NC} \sum_{y=1}^{NY} C_{i,t}^w P_{i,t,s,c,y}^w \right\} - \sum_{t=1}^{NT} \sum_{i=1}^{NB} \sum_{c=1}^{NC} \sum_{y=1}^{NY} C_{i,t}^G P_{i,t,c,y}^G \quad (14)$$

subject to

a) Equality Constraints: Active and Reactive Power Balance at Each Bus

$$\sum_{t=1}^{NT} \sum_{i=1}^{NG} P_{i,t,c,y}^G + \sum_{t=1}^{NT} \sum_{i=1}^{NB} P_{i,t,s,c,y}^w - \sum_{q=1}^{NQ} \sum_{i=1}^{NB} P_{i,q,s,y}^D = \sum_{j=1}^{NB} V_{i,s,c,y} V_{j,s,c,y} T_{ij} \{G_{ij} \cos(\delta_{i,s,c,y} - \delta_{j,s,c,y}) + B_{ij} \sin(\delta_{i,s,c,y} - \delta_{j,s,c,y})\} \quad (15)$$

$$\sum_{t=1}^{NT} \sum_{i=1}^{NG} Q_{i,t,c,y}^G + \sum_{t=1}^{NT} \sum_{i=1}^{NB} Q_{i,t,s,c,y}^w - \sum_{q=1}^{NQ} \sum_{i=1}^{NB} Q_{i,q,s,y}^D = \sum_{j=1}^{NB} V_{i,s,c,y} V_{j,s,c,y} T_{ij} \{G_{ij} \sin(\delta_{i,s,c,y} - \delta_{j,s,c,y}) - B_{ij} \cos(\delta_{i,s,c,y} - \delta_{j,s,c,y})\} \quad (16)$$

b) Inequality Constraints

-Branch flow constraints

$$\sqrt{(G_{ij}^2 + B_{ij}^2)(V_{i,s,c,y}^2 + \frac{V_{j,s,c,y}^2}{T_{ij}^2} - \frac{2V_{i,s,c,y} V_{j,s,c,y} \cos(\delta_{i,s,c,y} - \delta_{j,s,c,y})}{T_{ij}})} \leq I_{ij}^{\max} \quad (17)$$

-Voltage limits at each bus

$$V_i^{\min} \leq V_{i,s,c,y} \leq V_i^{\max} \quad (18)$$

$$\delta_i^{\min} \leq \delta_{i,s,c,y} \leq \delta_i^{\max} \quad (19)$$

-WTs generation constraint

$$0 \leq P_{i,t,s,c,y}^w \leq \gamma_{i,s,c}^w \times P_{i,rated}^w \quad (20)$$

$$Q_i^{w,\min} \leq Q_{i,t,s,c,y}^w \leq Q_i^{w,\max} \quad (21)$$

-Capacity constraints at substation

$$P_i^{G,\min} \leq P_{i,t,c,y}^G \leq P_i^{G,\max} \quad (22)$$

$$Q_i^{G,\min} \leq Q_{i,t,c,y}^G \leq Q_i^{G,\max} \quad (23)$$

B. ANM Schemes Incorporation

DNOs will be able to optimize using their assets with incorporation of ANM schemes by dispatching generation, controlling OLTCs and voltage regulators, controlling reactive power, and reconfiguring the system [5]. ANM implementations will need advanced control techniques while the actual actuation of devices (e.g., tap changers) will depend on their respective response time-scales.

1) Coordinated Voltage Control

By dynamically controlling the OLTC at the substation and the corresponding distribution secondary voltage, more DG capacity might be connected [28]. Thus, at each phase, the secondary voltage of the OLTC will be treated as a variable, rather than a fixed parameter, while keeping its value within the statutory range as follows:

$$T_{ij}^{\min} \leq T_{ij} \leq T_{ij}^{\max} \quad (24)$$

2) Adaptive Power Factor Control

Power factor of WTs can be controlled to maximize the dispatched energy of WTs. In practice, WTs require to meet the particular requirement depending on the regulation of the country. For instance, in the UK, the power factor of a WT should remain between 0.95 leading and 0.95 lagging [29-30]. Therefore, the following constraint applies:

$$\phi_i^{w,\min} \leq \phi_{i,s,c,y}^w \leq \phi_i^{w,\max} \quad (25)$$

C. Capability Curve of DFIG-based WTs

In steady state, the DFIG capability limits are obtained by considering the stator- and rotor-rated currents as well as calculating the total capacity limits of WT. These currents are related to stator and rotor heating because of Joule's losses. The capability curve of DFIG-based WTs is shown in Fig.4. More details about it can be found in [31].

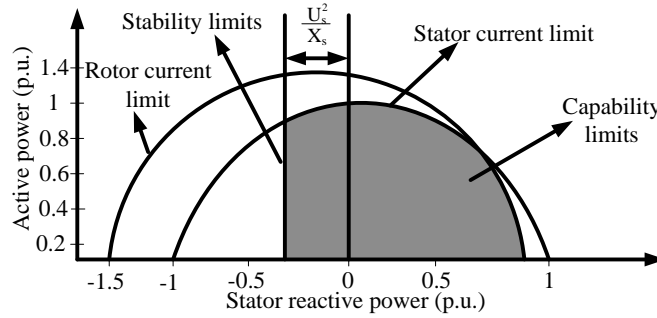


Fig.4. DFIG capability limits

VI. Case Study and Simulation Results

In this section, the distribution system used to test the proposed method is described. The following analyses are based on 33 kV 16-bus rural weakly meshed UKGDS whose data are available in [32]. The single-line diagram of the distribution system is shown in Fig. 5.

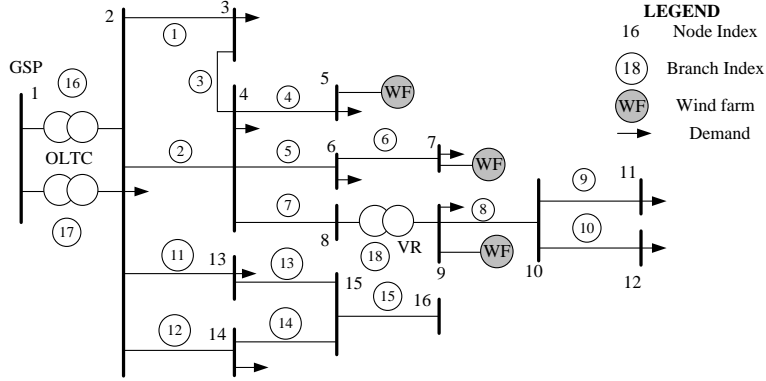


Fig.5. 16-bus UKGDS with candidate locations for WTs

The feeders are supplied by two identical 30-MVA 132/33 kV transformers. Two OLTCs, allocated between buses 1 and 2, has a target voltage of 1.05 p.u. at the secondary. A voltage regulator (VR) is located between buses 8 and 9, with the latter having a target voltage of 1.03 p.u.. Voltage limits are taken to be $\pm 6\%$ of nominal value, i.e. $V_{\min} = 0.94$ and $V_{\max} = 1.06$ p.u. and the power factor of WTs ranges from 0.95 leading to 0.95 lagging. In this paper, it is assumed that buses 5, 7 and 9 are three possible WTs locations but it is notable that the selection of possible WTs locations relies on non-technical factors such as legal requirements, space/land availability and other amenities. Four states for loads and six states for wind power generation are considered respectively by using Normal and Weibull PDFs. The probabilities of load and wind states are presented in Tables I and II, respectively. By incorporating these scenarios, as explained in Section IV, 24 combined wind-load states are obtained as given in Table III.

Table I. Load states and corresponding probabilities

State #	Load (%)	π_D
D_1	100.00	0.10
D_2	75.00	0.15
D_3	55.00	0.45
D_4	35.00	0.30

Table II. Wind states and corresponding probabilities

State #	Wind (%)	π_w
w_1	100.00	0.05
w_2	85.30	0.03
w_3	58.50	0.60
w_4	40.60	0.25
w_5	35.10	0.01
w_6	00.00	0.06

Table III. Combined wind and load states and corresponding probabilities

State #	Load (%)	Wind (%)	π_s
s_1	100.00	100.00	0.0050
s_2	100.00	85.30	0.0030
s_3	100.00	58.50	0.0600
s_4	100.00	40.60	0.0250
s_5	100.00	35.10	0.0010
s_6	100.00	00.00	0.0060
s_7	75.00	100.00	0.0075
s_8	75.00	85.30	0.0045
s_9	75.00	58.50	0.0900
s_{10}	75.00	40.60	0.0375
s_{11}	75.00	35.10	0.0015
s_{12}	75.00	00.00	0.0090
s_{13}	55.00	100.00	0.0225
s_{14}	55.00	85.30	0.0135
s_{15}	55.00	58.50	0.2700
s_{16}	55.00	40.60	0.1125
s_{17}	55.00	35.10	0.0045
s_{18}	55.00	00.00	0.0270
s_{19}	35.00	100.00	0.0150
s_{20}	35.00	85.30	0.0090
s_{21}	35.00	58.50	0.1800
s_{22}	35.00	40.60	0.0750
s_{23}	35.00	35.10	0.0030
s_{24}	35.00	00.00	0.0180

Three 15 MW wind farms (WFs) are installed at buses 5, 7 and 9. Each of them is composed of 5×3 MW WTs. It is assumed that maximum four WF's can be allocated at each candidate bus. For each scenario and configuration, this is represented by four equal blocks in the WF's offer with the same price. The planning horizon is assumed to be 5 years. The offer price at substation is assumed to be 160 £/MWh. Moreover, it is assumed that the offer price at the substation increases by 5% every year. Regarding the bids of loads, it is assumed that there are two blocks for each load as presented in Table IV at maximum load and the first year of the planning horizon. Also, it is assumed that the load growth is 5% for each year of the planning horizon. Table V presents all the possible multi-WT configurations for the three WF's locations using (1).

Table IV. Bid Quantity and Price in Planning Year 1

Bus No.	Quantity (MW)		Price (£/MWh)	
	Block 1	Block 2	Block 1	Block 2
2	3.00	2.50	350	300
3	1.10	0.93	350	300
4	0.06	0.06	300	300
5	11.00	8.20	250	250
6	1.06	0.90	400	300
7	0.30	0.25	450	250
9	0.95	0.95	400	300
10	1.70	1.00	325	275
11	2.15	0.70	250	250
12	0.42	0.39	250	225
13	0.51	0.50	200	200
14	0.38	0.20	300	300

Table V. Description of Multi-WT Configurations

Multi-configurations	WT status/location		
	Bus 5	Bus 7	Bus 9
1	1	0	0
2	0	1	0
3	0	0	1
4	1	1	0
5	1	0	1
6	0	1	1
7	1	1	1

A. Calculation of the WTs Offer Price From the Point of View of DNOs

In order to calculate the price of WTs' offers, financial data, i.e. WTs' life time, installation cost, depreciation time, interest rate, are considered as summarized in Table VI. The annual cost for WTs is calculated as follows [33-38]:

$$Ann_Cost = \frac{r(1+r)^n}{(1+r)^n - 1} \times Inst_Cost \quad (26)$$

where r is the interest rate, n is the depreciation period in years, $Inst_Cost$ is the installation cost, and Ann_Cost is the annual cost for depreciation. The capacity factor (CF) is evaluated according to the wind generation data and the WTs' capability curves. The offer price of WTs is calculated by dividing the annual costs by the number of equivalent hours as presented in Table VI. In order to investigate the impact of multi-WT configurations and ANM schemes on the SW, dispatched energy of WTs and D-LMP over the planning horizon, two scenarios are taken into account as presented in Table VII.

TABLE VI. Financial data for Calculating the offer price of 3-MW WT for the planning year 1

WTs size	3 MW
Installation cost (£/kW)	950
Depreciation time (years)	10
Interest rate (%)	3
Number of equivalent hours (h)	4000
Capacity factor (%)	46
Annual cost (£/kW-year)	334.10
WTs Offer Price (£/MWh)	27.84

TABLE VII. Scenarios

Scenarios	CVC	PFC	PF= 0.95 lagging
<i>A</i>	-	-	✓
<i>B</i>	✓	✓	-

Fig.6 shows the total dispatched energy of WFs over the planning horizon for each configuration and both scenarios. Configuration 2 (i.e. one WF at bus 7) has the lowest dispatched energy in all scenarios compared to other configurations while configurations 1 and 3 (i.e. one WF at buses 5 and 9, respectively) have the higher dispatched energy compared to that at bus 7. This is mainly due to the higher bid price and lower bid quantity (see Table IV) and voltage constraints at bus 7 compared to those at buses 5 and 9 as well as the thermal limits of the lines connecting the buses. Configuration 5 (i.e. two WFs at buses 5 and 9) has the higher dispatched energy compared to that in configurations 4 and 6. This is because of the higher bid quantity and lower bid price at buses 5 and 9 compared to those in configurations 4 and 6. It is seen that the dispatched energy in scenario *A* and configuration 4 (i.e. two WFs at buses 5 and 7) is almost equal to that in configuration 3 (i.e. one WF at bus 9). It is evident that

configuration 7 with three WFs installed at candidate buses has the highest dispatched energy compared to that in other configurations. It is seen from Fig. 6 that in scenarios *B* considering ANM schemes, higher active power can be dispatched by WFs compared to that in scenario *A*. The total dispatched energy for all configurations over the planning horizon at candidate buses in scenario *A* is shown in Fig.7. Assuming 5% load growth for each year over the planning horizon, the dispatched energy proportionally increases to the load growth at all candidate buses. For instance, at bus 9, the total dispatched energy for all configurations at the first year of the planning horizon is about 1700 MWh while it is 1900 MWh in the last year which increases about 13% compared to the first year.

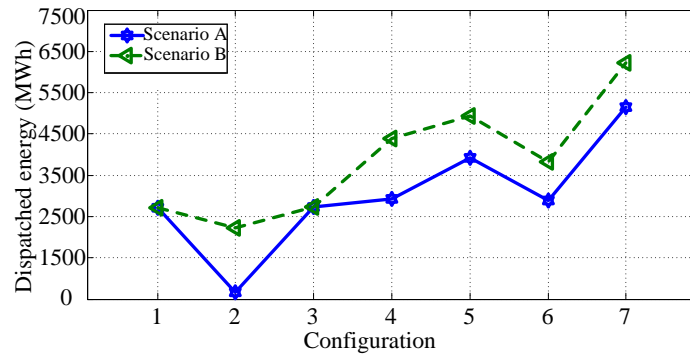


Fig. 6. Total dispatched energy for each configuration and over the planning horizon

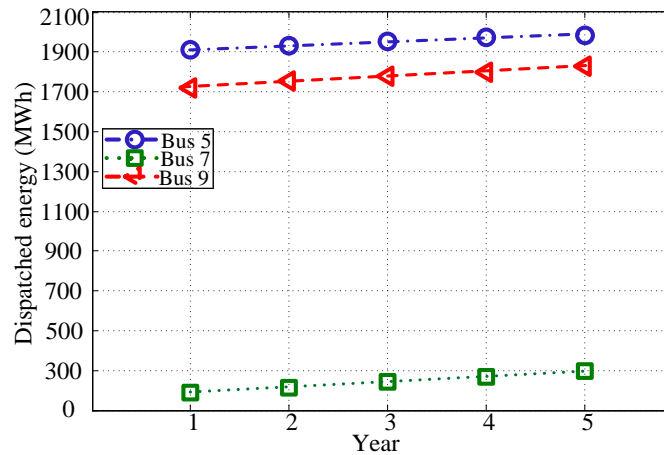


Fig. 7. Dispatched energy at each bus in Scenario A over the planning horizon

Fig. 8. shows the total SW for each configuration over the planning horizon. It is seen that configurations 2 and 7 respectively have the lowest and highest values of SW compared to others. This is mainly because of the lowest and highest dispatched energy at these configurations respectively as WTs allocation allows increasing the SW. The D-LMPs at candidate buses for each configuration in scenario *A* over the planning horizon is shown in Fig.9 (a). It is

observed that at bus 7 and configuration 2, the D-LMP has the highest value. This is mainly because of the lowest dispatched energy at this bus and configuration. It is seen that in scenario A, the D-LMP in configuration 3 at bus 9 is about 1500 £/MWh while this value in configuration 4 is about 1300 £/MWh. This is due to the almost equal dispatched energy at these configurations (see Fig.6 scenario A). Therefore, configurations 1, 3 and 5 are more economical than configurations 2, 4 and 6. Fig. 9 (b) shows the D-LMPs at candidate buses in scenario A over the planning horizon for each configuration. It is seen that bus 5 has the lowest D-LMP while bus 7 has the highest one which is because of the highest and lowest dispatched energy at buses 5 and 9, respectively. It can also be seen that the D-LMP proportionally decreases to load growth over the planning horizon due to the increment in the dispatched energy over the planning horizon.

As a result, the method can be used as a useful tool for DNOs to install WTs at more advantageous locations in terms of consumers' benefits and cost reduction considering network constraints and reliability. Also, by adopting ANM schemes, more wind power can be integrated into the grid compared to that in passive networks. This is achieved through D-LMPs to provide a real-time price to the end-user customers.

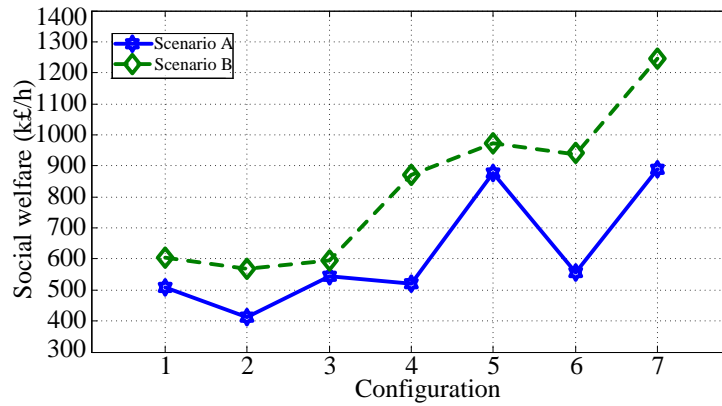


Fig.8. Total social welfare for each configuration over the planning horizon

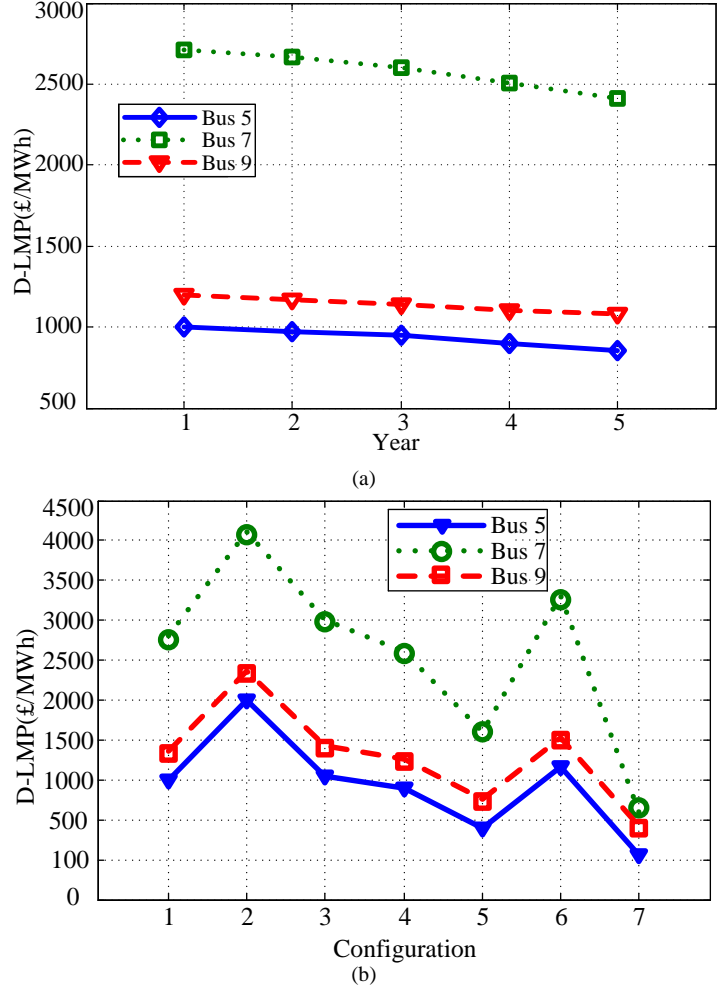


Fig.9. (a) D-LMP for each configuration at each bus in Scenario A and first year of planning horizon, (b) D-LMP at each bus in Scenario A over the planning horizon

B. Computational Issues

The proposed method has been implemented in GAMS and the non-linear program (NLP) solved using IPOPT solver [39] on a PC with Core i7 CPU and 16 GB of RAM. The computational burden of the proposed method is characterized in Table VIII.

To validate the results, the proposed method was also coded in the MATLAB environment and solved with IPOPT solver. The results obtained by MATLAB are very close (i.e. 2% error) to those obtained in GAMS.

Table VIII. Problem characterization

Variables	42458
Constraints	31782
Time (sec)	2442.7

VII. Conclusions

In this paper, a stochastic method for the planning of active distribution networks within a distribution market environment is proposed. The method considers capability curve of WTs, ANM schemes and multi-WT configurations. MMMOPF is used to maximize SW considering uncertainties related to wind speed and load demand. ANM is considered as an important means of increasing the capability of distribution networks to install renewable DGs. It is revealed that the multi-WT configurations under ANM schemes could increase the potential of wind power penetration at certain locations and consequently decreases D-LMPs throughout the network. It can be used as a tool for DNOs to evaluate the impact of wind power penetration on a given network in terms of technical and economic effects.

Acknowledgment

This work was supported in part by the SITARA project funded by British Council and the Department for Business, Innovation and Skills, UK and in part by the University of Bradford, UK under the CCIP grant 66052/000000.

REFERENCES

- [1] M. Gandomkar, M. Vakilian, and M. Ehsan, "Optimal distributed generation allocation in distribution network using Hereford Ranch algorithm," in Proc. Int. Conf. Electr. Mech. Syst., 2005, vol. 2, pp.916–918.
- [2] P. Siano, L. F. Ochoa, G. P. Harrison, A. Piccolo, "Assessing the strategic benefits of distributed generation ownership for DNOs," *IET Gener. Transm. Distrib.*, vol.3, no.3, pp. 225-236, 2009.
- [3] G. Mokryani, P. Siano, "Strategic placement of DNO owned wind turbines by using market-based optimal power flow", *IET Gener. Transm. Distrib.*, vol.8, no.2, pp.281-289, 2014.

- [4] R. C. Dugan, T. E. McDermott, and G. J. Ball, "Planning for distributed generation," *IEEE Ind. App. Mag.*, vol. 7, no. 2, pp. 80–88, 2001.
- [5] P. Djapic, C. Ramsay, D. Pudjianto, G. Strbac, J. Mutale, N. Jenkins, and R. Allan, "Taking an active approach," *IEEE Power Energy Mag.*, vol. 5, no. 4, pp. 68–77, 2007.
- [6] S. N. Liew and G. Strbac, "Maximising penetration of wind generation in existing distribution networks," *IEE Gener. Transm. Distrib.*, vol. 149, no. 3, pp. 256–262, 2002.
- [7] P. Siano, P. Chen, Z. Chen, and A. Piccolo, "Evaluating maximum wind energy exploitation in active distribution networks," *IET Gener. Transm. Distrib.*, vol. 4, no. 5, pp. 598–608, 2010.
- [8] G. Mokryani, P. Siano, A. Piccolo, "Optimal allocation of wind turbines in microgrids by using genetic algorithm," *Journal of Ambient Intelligence and Humanized Computing*, vol. 4, no. 6, pp. 613–619, 2013.
- [9] R. Palma-Behnke, J. L. A. Cerda, L. Vargas, and A. Jofre, "A distribution company energy acquisition market model with the integration of distribution generation and load curtailment options," *IEEE Trans. Power Syst.*, vol. 20, no. 4, pp. 1718–1727, 2005.
- [10] R. A. F. Currie, G. W. Ault, R. W. Fordyce, D. F. MacLeman, M. Smith, and J. R. McDonald, "Actively managing wind farm power output," *IEEE Trans. Power Syst.*, vol. 23, no. 3, pp. 1523–1524, 2008.
- [11] O. Samuelsson, S. Repo, R. Jessler, J. Aho, M. Karenlampi, and A. Malmquist, "Active distribution network—Demonstration project ADINE," in *Proc. IEEE PES Innovative Smart Grid Technologies Conf. Europe (ISGT Europe)*, Oct. 2010.
- [12] M. J. Dolan *et al.*, "Distribution power flow management utilizing an online optimal power flow technique," *IEEE Trans. Power Syst.*, vol. 27, no. 2, pp. 790–799, 2012.
- [13] F. Pilo, G. Pisano, and G. G. Soma, "Optimal coordination of energy resources with a two-stage online active management," *IEEE Trans. Ind. Electron.*, vol. 58, no. 10, pp. 4526–4537, 2011.
- [14] S. L. Hay, G.W. Ault, K. R.W. Bell, and J. R. McDonald, "System operator interfaces to active network management schemes in future distribution networks," in *Proc. 43rd Int. Universities Power Eng. Conf. (UPEC)*, Sep. 2008.
- [15] A. Shafiu, T. Bopp, I. Chilvers, and G. Strbac, "Active management and protection of distribution networks with distributed generation", in *Proc. IEEE Power Eng. Soc. General Meeting*, 2004.
- [16] R. Hidalgo, C. Abbey, and G. Joos, "Technical and economic assessment of active distribution network technologies," in *Proc. IEEE Power Energy Soc. General Meeting*, 2011.
- [17] Z. Hu and F. Li, "Cost-benefit analyses of active distribution network management, part I: Annual benefit analysis," *IEEE Trans. Smart Grid*, vol. 3, no. 3, pp. 1067–1074, Sep. 2012.
- [18] H. Falaghi and M. R. Haghifam, "ACO based algorithm for distributed generation sources allocation and sizing in distribution systems," in *Proc. IEEE Power Tech*, 2007, pp. 555–560.
- [19] Y. M. Atwa and E. F. El-Saadany, "Probabilistic approach for optimal allocation of wind-based distributed generation in distribution systems" *IET Renew. Power Gener.*, vol. 5, no. 1, pp. 79–88, 2011.
- [20] H. M. Ayres, W. Freitas, M. C. De Almeida, and L. C. P. Da Silva, "Method for determining the maximum allowable penetration level of distributed generation without steady-state voltage violations," *IET Gener. Transm. Distrib.*, vol. 4, no. 4, pp. 495–508, 2010.

- [21] A. A. Tamimi, A. Pahwa, and S. Starrett, "Effective wind farm sizing method for weak power systems using critical modes of voltage instability," *IEEE Trans. Power Syst.*, vol. 27, no. 3, pp. 1610–1617, 2012.
- [22] D. J. Burke and M. J. O'Malley, "Maximizing firm wind connection to security constrained transmission networks," *IEEE Trans. Power Syst.*, vol. 25, no. 2, pp. 749–759, 2010.
- [23] T. H. M. El-Fouly, H. H. Zeineldin, E. F. El-Saadany, and M. M. A. Salama, "Impact of wind generation control strategies, penetration level and installation location on electricity market prices," *IET Renew. Power Gener.*, vol. 2, no. 3, pp. 162–169, 2008.
- [24] M. Zhao, Z. Chen, and F. Blaabjerg, "Probabilistic capacity of a grid connected wind farm," in *Proc. 31st IEEE Annu. Conf. Industrial Electronics Society (IECON)*, 2005, pp. 774–779.
- [25] A. Rabiee, A. Soroudi, B. Mohammadi-Ivatloo, M. Parniani, "Corrective voltage control scheme considering demand response and stochastic wind power", *IEEE Trans. Power Syst.*, vol. 29, no. 6, pp. 2965 - 2973, 2014.
- [26] A. Rabiee, A. Soroudi, "Stochastic multiperiod OPF model of power systems with HVDC-connected intermittent wind power generation", *IEEE Trans. Power Syst.*, vol. 29, no. 1, pp. 336–344, 2014.
- [27] P. Siano, G. Mokryani, "Evaluating the benefits of optimal allocation of wind turbines for distribution network operators", *IEEE Syst. J.*, vol.9, no.2, pp.629-638, 2015.
- [28] G. Mokryani, A. Majumdar, B.C. Pal, "Probabilistic Method for the Operation of Three-Phase Unbalanced Active Distribution Networks", *IET Renew. Power Gener.*, vol.10, no.7, pp.944-954, 2016.
- [29] M. Tsili, S. Paphanssiou, "A review of grid code technical requirements for wind farms, *IET Renew. Power Gener.*, vol.3, no.3, pp. 308-332, 2009.
- [30] P.N. Vovos, A.E. Kiprakis, A.R. Wallace, and G.P. Harrison, "Centralised and distributed voltage control: impact on distributed generation penetration", *IEEE Trans. Power Syst.*, vol.22, no.1, pp. 476-483, 2007.
- [31] G. Mokryani, P. Siano, A. Piccolo, Zhe Chen, "Improving fault ride-through capability of variable speed wind turbines in distribution networks", *IEEE Syst. J.*, vol.7, no.4, pp.713-722, 2013.
- [32] Distributed Generation and Sustainable Electrical Energy Centre. United Kingdom Generic Distribution System (UKGDS). [Online]. Available: <http://www.sedg.ac.uk>.
- [33] A. G. Tsikalakis and N. D. Hatziargyriou, "Centralized control for optimizing microgrids operation," *IEEE Trans. Energy Convers.*, vol. 23, no. 1, pp. 241–248, 2008.
- [34] P. Siano, G. Mokryani, "Evaluating the Benefits of Optimal Allocation of Wind Turbines for Distribution Network Operators", *IEEE Syst. J.*, vol.9, no.2, pp.629-638, 2015.
- [35] G. Mokryani, P. Siano, "Evaluating the Integration of Wind Power into Distribution Networks by using Monte Carlo Simulation", *Int. J. Electrical Power and Energy Syst.*, vol. 53, pp.244-255, 2013.
- [36] P. Siano, G. Mokryani, "Assessing Wind Turbines Placement in a Distribution Market Environment by Using Particle Swarm Optimization", *IEEE Trans. Power Syst.*, vol.28, no.4, pp.3852-3864, 2013.
- [37] G. Mokryani, P. Siano, "Combined Monte Carlo Simulation and OPF for Wind Turbines Integration into Distribution Networks", *Electr. Power Syst. Res.*, vol.103, pp.37-48, 2013.

- [38] G. Mokryani, P. Siano, "Optimal Wind Turbines Placement within a Distribution Market Environment", *Applied Soft Computing*, vol.13, no.10, pp. 4038-4046, 2013.
- [39] A. Brooke, D. Kendrick, A. Meeraus, R. Raman, "GAMS A User's Guide", GAMS Development Corporation, Washington DC, 1998.